



# Characterizing global equatorial sporadic-E layers through COSMIC GNSS radio occultation measurements

Aramesh Seif<sup>1</sup> · Sampad Kumar Panda<sup>2</sup>

Received: 24 November 2023 / Accepted: 10 June 2024 / Published online: 14 June 2024  
© The Author(s), under exclusive licence to Springer Nature B.V. 2024

## Abstract

The Global Navigation Satellite System Radio Occultation (GNSS-RO) technique has proven to be a powerful tool for studying E-region irregularities, i.e., Sporadic E (Es) which is primarily associated with the amplitude and phase scintillations. In the present study, an extensive 7-year GNSS-RO scintillation indices data from the Constellation Observing System for Meteorology, Ionosphere, and Climate (COSMIC) observations was employed to investigate the global distribution and seasonal variation of the Es occurrences under solar activity near the magnetic dip equator. Our analysis from the Earth's magnetic field parameters such as horizontal intensity and inclination estimated by the International Geomagnetic Reference Field model (IGRF) reveals that Earth's magnetic field plays a crucial role in determining the global distribution of Es layers. Moreover, the abundance of Es shows a clear dependence on season/longitude, and the occurrence statistics of Es are closely aligned with the earlier reports. The solar activity dependence of the Es occurrence characteristics demonstrates its significant reduction with increased solar activity for most of the seasons in all longitude sectors. We address the Gradient Drift instability as a source mechanism of the Es layer's appearance at the magnetic dip equator, where wind shear theory fails to operate because of the minimal inclination of the geomagnetic field.

**Keywords** Ionospheric scintillation · Sporadic E layer · GNSS radio occultation · Plasma instability

## 1 Introduction

The Earth's ionosphere, a region of the upper atmosphere extending from approximately 50 to 1000 kilometers above the Earth's surface, plays a crucial role in global communication, navigation, and weather prediction (Langley 2000). Understanding the complex dynamics of the ionosphere is of paramount importance for various technological applications and scientific endeavors. During the last three decades, significant advancements in understanding and modeling various ionospheric parameters/phenomena such as electron density, equatorial wind and electrodynamics, ionospheric TEC gradients, equatorial spread-F (ESF), scintillation indices, and sporadic E layers under varied seasons, solar and geomagnetic conditions and their altitudinal and latitudinal

variations (Arras et al. 2008; Jiao et al. 2017; Resende et al. 2018b; Huang 2018; Li et al. 2020; Qiu et al. 2021; Tang et al. 2022; Emmons et al. 2023; Fontes et al. 2024). One intriguing phenomenon that occurs within this dynamic region is the sporadic E (Es) layer. Es is a sporadic and localized enhancement of electron density within the ionosphere, typically occurring in the E region, which lies at an altitude of 90 to 120 kilometers with a thickness of 0.5 – 5 km and a horizontal extent of 10-1000 km (Whitehead 1970; Yakovlev et al. 2008). These thin sheet layers are called Es layers because of their apparent intermittent appearances in time and space. As per earlier literature, Es layers underwrites about more than 30% of the ionospheric irregularities that can affect the signal tracking performance in the global positioning system (GPS)/global navigation satellite system (GNSS) based operations (Yu et al. 2020). Such transient electron density structures can drastically affect other radio wave propagation, leading to ionospheric scintillations (Seif et al. 2017, 2015, 2012; Zou and Wang 2009) and acute fading of the signals to cause temporary interruption or even loss of lock in satellite-based communication and navigation systems (Mao et al. 2018; Vankadara et al. 2022). Studying

✉ A. Seif  
arameshseif@gmail.com

<sup>1</sup> Department of Physics, Shahid Beheshti University, Evin, Tehran 1983969411, Iran

<sup>2</sup> Department of ECE, Koneru Lakshmaiah Education Foundation, Vaddeswaram, Andhra Pradesh 522302, India

the characteristics and behavior of sporadic E is essential for improving the reliability and accuracy of modern technological systems relying on trans-ionospheric radio propagation services. The wind-shear theory is the most common theoretical explanation for the formation of Es layers (Whitehead 1989). According to this theory, mainly the east-west neutral wind due to tides or gravity waves moves the ions vertically in the E region ionosphere. Vertical shear in this wind, in the correct sense, compresses the ions into a thin, patchy sheet layer (Whitehead 1989, 1970). The theory has proven to work well in the mid-latitude, where the magnetic inclination angle is steep enough to produce Es layers (Collinson et al. 2020; Fujita et al. 1978; Hajkowicz 1978, 1977; Hajkowicz and Minakoshi 2003; Ogawa et al. 1989; Sinno 1980; Whitehead 1989, 1970). In equatorial regions, almost no Es layers are observed due to the strong magnetisation of the electrons associated with the exactly horizontal field lines, thereby not allowing the electrons to follow the converging ions moving with the neutral wind (Arras and Wickert 2018). Rather, the Es layers are believed to have a strong correlation with the plasma irregularities under EEJ conditions whereas during certain CEJ days, the Es layer turns into a temporary blanketing Es layer (Esb) that could be associated with the equatorial electrojet current plasma instabilities, mainly the gradient drift instability, also known as Type II irregularity (Dhanya et al. 2008; Forbes 1981; Resende et al. 2016; Tsunoda 2008; Whitehead 1989, 1963). However, the polar latitudes are accompanied by two types of Es: a) thin-layered Es formations with less electron density related to wind shear and b) thick-layered Es formations with increased electron density corresponding to high energy particle precipitation associated with intensive shock waves of the solar wind (Yakovlev et al. 2010). The concentration of Es ions in this region is effectively achieved through the action of convection electric fields and the vertical movement of gravity waves. This process is highly efficient according to studies conducted by Kirkwood and Nilsson (2000) as well as MacDougall et al. (2000a, 2000b). According to the wind-shear theory, an Es layer will not form when the inclination angle becomes too small which implies that intense Es layers are hardly expected at the magnetic dip equator. Nevertheless, previous studies conducted in the low latitude and equatorial regions suggest the appearance of Es and show the occurrence of Es is associated with daytime scintillation (Alfonsi et al. 2013; Huang 1978; Kumar et al. 2007; Patel et al. 2009, 2007; Seif et al. 2017, 2015, 2012; Zou 2011; Zou and Wang 2009). The question arises as to what are the source mechanism and the physical processes that lead to the appearance of daytime Es at the magnetic dip equator, where the inclination angle is zero and the wind-shear theory does not work. To address this question, the present study provides an analysis of RO data covering the global equatorial regions and presents the possible physical

processes and source mechanisms of the Es at the magnetic dip equator. The climatology of Es has been the subject of significant research efforts in recent decades (Axford 1963; Haldoupis 2011; Hodos et al. 2022; Tsai et al. 2018; Whitehead 1961; Wu et al. 2005; Yamazaki et al. 2022) and has become a rising important issue with the increased reliance on trans-ionospheric signals for global communication and navigation applications that are vulnerable to ionospheric plasma instability. Traditionally, the observation techniques for studying Es include ground-based ionosondes and incoherent scatter radar, measurements from which show significant variations in midlatitude Es occurrence, with peak activity during daytime hours and summer months (Chandra and Rastogi 1975; Devasia 1976; Dhanya et al. 2008; Farley 1985; Hocke et al. 2001; Kelly 2012; Mathews 1998; Mathews and Bekeeny 1979; Oyinloye 1971; Reddy and Devasia 1977; Whitehead 1989, 1970). The first global map of the occurrence of Es layers was produced by Leighton et al. (1962) by employing available ionosonde data through a meridional chain of stations. However, it has been difficult to understand the global Es layer and its evolution mechanism due to sparse coverage of the parameter with the limited number of worldwide ground-based observatories.

In recent years, significant advancements have been made in observation and measuring techniques for detecting the presence of Es layers. Satellite-to-satellite radio communications, particularly GPS-LEO (Global Positioning System-Low Earth Orbiter) occultations, offer an ideal setup for observing layered structures such as Es providing numerous advantages over sparse coverage and limited threshold limit of ground-based observation techniques (Panda et al. 2021; Yu et al. 2020). For example, ground-based GPS receivers typically require over-horizon measurements to observe Es layers (Coco et al. 1995), but these measurements are often affected by large multipath errors. In contrast, satellite-to-satellite links generally do not encounter multipath issues. This means that multipath usually occurs in the troposphere where the gradients especially of the water vapour are very strong (e.g., Liu et al. 2015). But it can also appear at ionospheric heights (e.g., Yue et al. 2016). It is not a frequent issue but it appears in line with ionospheric irregularities and space weather events. And, can adequately resolve thin-layered structures with high-rate vertical sampling using advanced GPS receivers at frequencies of 50 Hz and 100 Hz. Additionally, satellite-to-satellite links offer stronger Es signals compared to ground-to-satellite links and are less susceptible to contamination from F region fluctuations. Furthermore, while GPS-ground measurements are limited to regional observations, GPS-LEO occultations provide global coverage, generating approximately 2000 daily profiles using a single antenna. The GNSS RO system comprises approximately 29 satellites, with 24 functioning and a few spare satellites, arranged in six circular

orbital planes at an altitude of around 20,200 km with an inclination of 55 degrees. These satellites continuously transmit signals at two primary L-band frequencies: 1.6 GHz (L1) and 1.2 GHz (L2) (Spilker 1978). Given the vast amount of GNSS RO data available, it is now possible to gain a deeper understanding of the characteristics of sporadic E near the magnetic dip equator.

While significant research has been conducted on Es morphology using GNSS RO data, previous studies have primarily focused on mid-latitude regions. For example, Chu et al. (2014) utilized measurements from COSMIC RO and the HWM07 model to investigate the correlation between the spatial and temporal distribution of Es occurrence rates and the simulated divergence of vertical Fe<sup>+</sup> flux. They discovered that the seasonal variations in Es occurrence rates are likely to be caused by the convergence of metal ion flux driven by vertical wind shear that descends under the influence of diurnal and semidiurnal tides. Referring to the fundamental role of the atmospheric tides (diurnal, semidiurnal, terdiurnal, and quarterdiurnal) on the formation and descent of Es layers, it is often termed as the “tidal ion layers” (Haldoupis and Pancheva 2006; Mathews 1998). Shinagawa et al. (2017) determined the Vertical Ionization Convergence (VIC) based on simulations of neutral wind and suggested that the simulated VIC could partially account for the geographical and seasonal variations observed in Es occurrence rates. Yu et al. (2019) conducted a comparison between the distributions of Es intensity and the divergence of vertical ion velocity. They observed that wind shear can explain the seasonal dependency of Es intensity within the altitude range of 97–114 km, but it becomes challenging to explain the patterns at higher altitudes. Detailed analyses of the distributions of RO-derived Es occurrence rates near the magnetic dip equator regions and their associated diurnal variations remain limited. Arras et al. (2022) used GNSS RO, Swarm, and Ionosonde data to study the altitude occurrence of Es layers at equatorial region. They found strong altitude and longitude dependence of equatorial electric field on low latitude sporadic E formation. However, they did not study the global investigation of Es layer. Hodos et al. (2022) recently developed an updated global climatology of Es with a huge datasets from GNSS RO and soundings 46 ionosonde across the globe during the period 2006–2019 that provides a clear picture of Es occurrence rates in terms of local time, season, intensity under quiet geomagnetic conditions. Researchers also attempted to model the global Es layer based on GNSS RO observables during the previous decade, but those are limited to climatological representation of the parameter (Niu and Fang 2023; Yu et al. 2022).

Despite the previous research have provided a rough explanation of the distribution and seasonal variation of Es layers through data observation, modeling and physical explanations through various theories, there is still limited under-

standing regarding the diurnal variation and altitude distribution of these layers near the magnetic dip equator. While Es has been widely investigated in different regions of the world, its behavior near the magnetic dip equator remains relatively unexplored as a major portion of the region falls in the oceans and a limited number of ground-based observatories are established so far along the equatorial landmass. The magnetic dip equator is the region on Earth where the geomagnetic field lines are parallel to the Earth’s surface. It exhibits unique characteristics due to the complex interplay between the Earth’s magnetic field and the equatorial ionosphere, the effects of which are mostly observed within  $\pm 15^\circ$  from the dip equator, widely known as the equatorial ionization anomaly (EIA) region (Timoçin et al. 2020). However, the lack of comprehensive studies focusing on Es in the EIA region has limited our understanding of this intriguing phenomenon in this specific region. Hence, the knowledge of the evolution and development of Es in the equatorial region is important for understanding the atmospheric dynamics and solar-terrestrial interactions.

In this study, we use the GNSS RO observables from Constellation Observing System for Meteorology, Ionosphere, and Climate (COSMIC) constellation of satellites, to detect the occurrence of Es layers along the magnetic dip equator in four regions: America, Africa, Asia, and Pacific. The observations using the RO techniques presented in this paper are essential to present the comprehensive global properties of Es along the magnetic dip equator ultimately to understand the source mechanism and the physical processes of Es formation where wind shear theory fails to operate. This study contributes to the development of space weather prediction, development of advanced satellite-based communication, early warning systems for ionospheric disturbances, and various astronomical science applications. The remaining part of this article is organized as follows. Section 2 introduces the dataset and the method that we used in this study. Section 3 presents the analysis results including the global occurrence of Es as a function of longitude, latitude, and a global map of it. Section 4 proposes the physical processes and generation mechanism of Es at the magnetic dip equator. The conclusion is given in Sect. 5.

## 2 Data and methodology

The principal instruments used in this study are the low Earth orbiting (LEO) COSMIC satellites that record ionospheric soundings using RO of the GPS signals (Jeng-Shing Chern and Huang 2013; Juang et al. 2013; Rocken et al. 2000). Each of the LEOs tracks the GPS satellites as they are occulted behind the Earth’s limb to retrieve up to 2000 daily profiles of key ionospheric properties (Rocken et al. 2000). Radio occultation is a limb-viewing innovative technique for atmospheric and lower ionospheric observations

with global coverage and high vertical resolution. The global coverage is approximately 2000 soundings per day retrieved from GPS-RO data along the GPS-LEO radio links near the ray path tangent points. The time series of the amplitude scintillation (S4 index) for each RO event is recorded by the COSMIC Data Analysis and Archive Center (CDAAC) in their level b1, which University Corporation manages for Atmospheric Research (UCAR), Colorado, United States of America. The dataset analyzed in this study is available by CDAAC as “scnLv1” that corresponds to the Level-1b scintillation data. The onboard algorithm of the GPS RO receiver does not measure the S4 index directly but measures the signal-to-noise intensity (square of SNR) fluctuations from the raw L1 amplitude measurements at 50 Hz sampling rate which are recorded at 1 Hz rate for minimizing the data volume. In brief, the raw scintillation output from the receiver is root mean square (RMS) SNR intensity fluctuation over one second (1 sec) and mean SNR intensity sampled at 50 Hz during the above period from which the S4 index is reconstructed at CDAAC ground processing unit. According to the CDAAC documentation ([http://cdaac-www.cosmic.ucar.edu/cdaac/doc/documents/s4\\_description.pdf](http://cdaac-www.cosmic.ucar.edu/cdaac/doc/documents/s4_description.pdf)), the ground processing involves the consideration of the SNR being following a Gaussian distribution due to scintillation and thereby applying a low pass filter to the time series of 1 sec averaged intensity for resulting in reconstruction of a long-term detrended S4 scintillation index. Hence, the amplitude scintillations contain information on the existence of Es as well as their altitude and intensity. The downloaded CDAAC global data files provide the maximum and minimum values of S4 (S4max and S4min), the average S4 over the 9 s around S4max (S4max9sec) during an occultation period (typically 1-15 minute), along with other parameters like geographic latitude, longitude, altitude as well as local time of the LEO satellite and tangent point (TP) positions during the S4max detection. In this study, we used the global S4max9s data in our analysis to avoid any spurious outlier in the 1 Hz S4 distribution. A detailed description of the procedure followed for preprocessing and extracting the S4 index is provided in earlier literature (Brahmanandam et al. 2012; Ko and Yeh 2010; Li et al. 2020). To investigate the comprehensive characteristics of Es in the vicinity of the magnetic dip equator, we use the scintillation GNSS COSMIC RO data between 2007 and 2013. To avoid the effects of magnetic disturbances in the analysis, only the geomagnetically quiet days are considered in this study by discarding the days having geomagnetic Kp index below 3 units (Kp < 3). The amplitude scintillation index can be calculated from the signal-to-noise ratio (SNR) observables following the earlier literature (Syndergaard 2006; Ko and Yeh 2010; Li et al. 2020) as shown in equation (1).

$$S4max9s = \frac{\sqrt{\langle (I - \langle \bar{I} \rangle)^2 \rangle}}{\langle \bar{I} \rangle} \quad (1)$$

Where S4 index was computed from the raw SNR measurements. “I” denote the square of SNR, and the brackets present the average taken over 9 s intervals.

Having nine-second values of  $\langle I \rangle$ , a low pass filter can be applied to a time series of these values to obtain a new average of the intensity at 9 seconds (Syndergaard 2006). The tangent point location for each RO data when the maximum S4 was measured are listed as follows, “alttp S4max”, “lcttp S4max”, “lattp S4max”, and “lontp S4max” parameters that represent the altitude, local time, latitude, and the longitude, respectively. The fluctuations in electron density within the ionosphere, which can be detected through scintillations in GPS signals, have a direct connection to the presence of ionospheric Es layers. Previous studies have utilized this relationship to detect and study these Es layers (Arras 2010; Chu et al. 2014; Yu et al. 2019). In this study, a threshold of 0.3 is established for analysis of the scintillation index (S4max) values from RO data. This criterion identifies the S4max values between 90 and 120 km that exceed 0.3 as being associated with Es layers, specifically indicating the presence of strong Es layers. The weakness of the above 50 Hz data used in this study is that no information can be obtained above ~120 km and hence it is hardly possible to find Es layers at higher altitudes as it might be influenced by other factors like meridional winds or descending intermediate layers at such height (Arras et al. 2009). The considered threshold value of S4max aligns with the thresholds used in previous studies (Carter et al. 2013; Seif et al. 2017; Yue et al. 2015). For further details of the Es occurrence, the readers may refer to Figs. 3- and 4-page 1573 of Seif et al. (2017). Earlier comparison studies of Yu et al. (2020) at low and middle latitude ionosonde stations with nearly a decadal datasets (from 2006 to 2014) emphasizes the use of COSMIC RO data for global Es layer measurements. Similar studies have been conducted by Resende et al. (2018a) in the Brazilian region reporting good agreement of RO derived Es layer characteristics with those from the coincident digisonde observations.

The data processing procedure is depicted in Fig. 1, showcasing a simplified overview. Following that, extracting all the eligible S4max values and identifying the Es-related values between 2007 and 2013.

### 3 Results

Using a comprehensive dataset spanning seven years, this study enables a further understanding of the characteristic occurrence of Es during both the solar minimum and maximum periods. The initial phase of the analysis involves plotting the magnetic inclination angle, also known as the “magnetic dip angle,” which is obtained from the International Geomagnetic Reference Field (IGRF) model (Macmillan



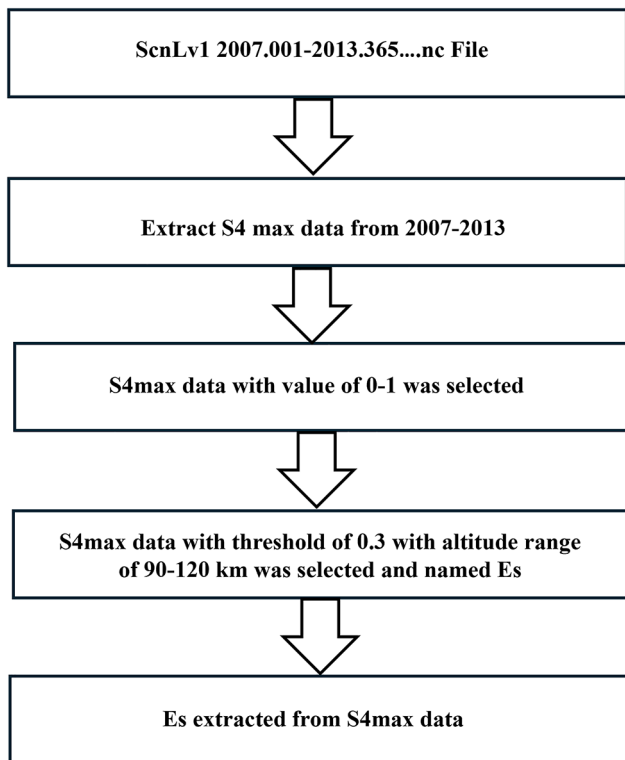


**Fig. 1** A flowchart that presents the process for calculating Es occurrence using RO data

and Maus 2005), against Local Time (LT). Moreover, the study examines the dependence of altitudinal, seasonal, and longitudinal variations of Es. Finally, the study investigates the impact of solar maximum on the Es identified by the COSMIC satellite.

### 3.1 The altitude distribution of Es in COSMIC data

The occurrence of Es for different altitudes and dip angles for four distinct seasons is presented in Fig. 2. As can be seen from the Fig. 2, the summertime Es is governing at an altitude range of 90–120 km with the peak around 105 km between 25°–60° dip angle. This is consistent with the previous study, as it shows the maximum occurrence of Es is in the summer time (Wu et al. 2005; Arras et al. 2008; Li et al. 2020). During the March equinox months and December, the altitude of occurrence of Es is observed at slightly lower altitude than the summer case, where irregularities form at an altitude range of 100–105 km. The rate of metallic ions is higher during summer than in winter due to the higher level of UV radiation (Whitehead 1989). Figure 3 presents the seasonal Es occurrence as a function of the magnetic dip angle. As can be seen from Fig. 3, the Es is scattered around 90 to 120 km with relatively lesser amplitude around the magnetic dip. However, it is often difficult to determine the exact altitude which needs further analysis with supportive datasets.

### 3.2 Occurrence of Es dependence on season and longitude

To study the seasonal longitudinal dependence of the occurrence of Es using RO data, we used the seven-year F-3/COSMIC datasets that were sorted into four seasons (March equinox: February, March, and April; June solstice: May, June, and July; September equinox: August, September, and October; December solstice: November, December, and January). The longitudinal sectors are divided into four regions, namely American (110°W to 20°W), African (20°E to 70°E), Asian (70°E to 160°E), and Pacific (160°E to 110°W). Figure 4 shows the result of this data sorting. This further data sorting reveals a strong dependence of the dip angle–LT distributions on longitude and season. The equatorial and winter–hemispheric Es are dominated by a diurnal variation, with the peak in the late afternoon (Chandra and Rastogi 1975; Devasia 1976). The Es percentage occurrence is calculated for  $s4max9s \geq 0.3$  between 0600 and 1800 LT and between 0–50° magnetic dip angles. The highest Es occurrences were in the Asian sector during June (summer). Overall, the fewest occurrences of Es were detected in the American and Pacific regions for all times of the year, except for the summer solstice, when the least Es occurrences were detected in the American region.

### 3.3 Es occurrences dependence on magnetic dip-angle

In order to show the occurrence of sporadic E layers on the map, we first study the occurrence of Es as a function of Geographic latitude, dip latitude, and dip angle (inclination angle), as shown in Fig. 5. It can be seen from Fig. 5 that scintillation (S4 index) as a function of inclination angle is wider and shows it depends on inclination angle. Please note that the occurrences of Es that we considered in our analysis also shown in Fig. 5 occurred between 90 and 120 km. This is consistent with the results obtained by Wu et al. (2005), who showed the global coverage of Es occurrence, diurnal, and seasonal variations of it, and presented that their activities depend on geomagnetic dip angle.

The GNSS RO measurements provide global maps of Es with a high vertical resolution. Figure 6 shows the first long-term series of Es occurrence derived by GNSS RO data from 2007 to 2013. It also represents a higher spatial resolution compared to earlier maps. To clearly show the occurrence of Es at the magnetic dip equator, we plotted the occurrence of Es as a function of the inclination angle with the focus at the magnetic dip equator in Fig. 7. The main features that can be obtained from Figs. 6 and 7 are (1) the distribution of Es around the Earth shows the abundance of Es over Southeast Asia compared to its scarcity over Africa and America sectors, and (2) the occurrence of Es at the magnetic dip

**Fig. 2** Seasonal occurrence of Es in Altitude-dip angle detected with COSMIC. The plot for the top right is June solstice (May, June, July), top left is December solstice (November, December, January). The plot at the bottom right represents the September equinox (August, September, October), whereas the bottom left denotes March equinox (February, March, April)

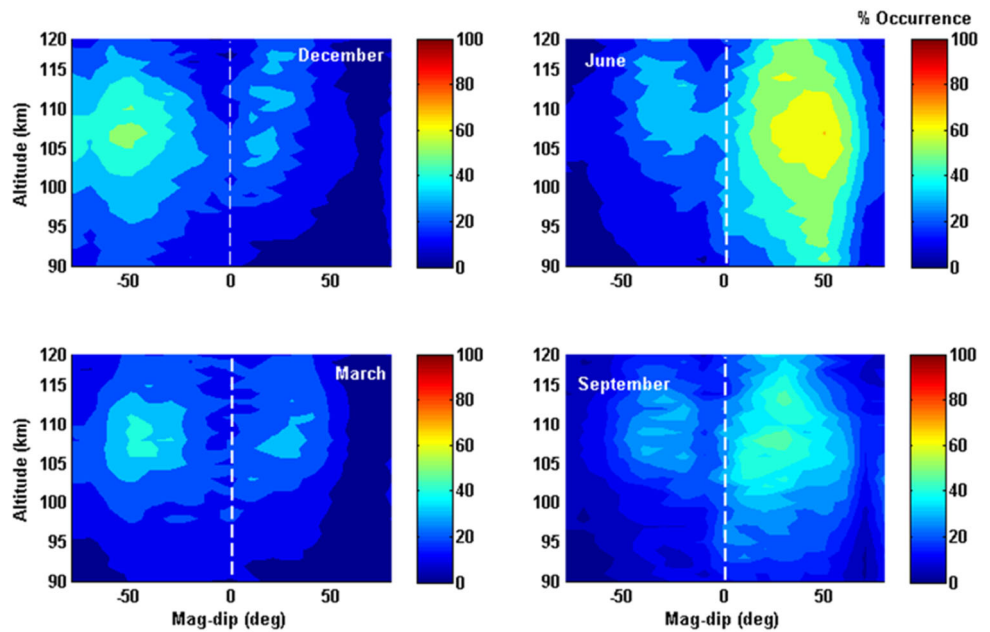
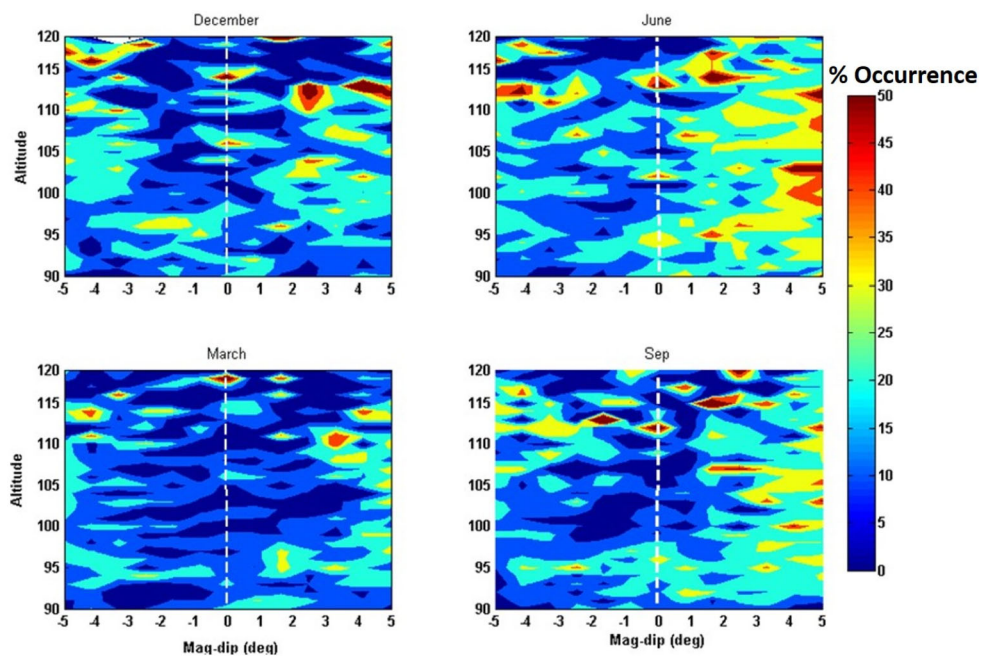


**Fig. 3** Seasonal Es occurrence in the altitude-dip angle at the magnetic dip equator detected with F-3/COSMIC. The layout in the plot is similar to Fig. 2



equator. Earlier studies show that over Southeast Asia, the wind pushes the ions and particles together more than over Africa and American sectors because the horizontal component of the Earth's magnetic field is more significant (Whitehead 1989, 1970). The rate of metallic ion production is thus greater over Southeast Asia and Es production is more effective. Again, the effect of a few more ions initially can lead to more abundant Es. In fact, the theory suggests that the compression mechanism is most effective in regions, where the horizontal component of the Earth's magnetic field ( $B_h$ ) is largest. In Southeast Asia, where  $B_h$  reaches its maximum,

sporadic E is highly intense compared to any other location on Earth. Conversely, in South Africa, where  $B_h$  is at its minimum, sporadic E is quite uncommon, even during the summer (Whitehead 1989, 1970).

### 3.4 Es occurrences dependence on solar activity

To understand how the occurrence of the sporadic E layer in the ionosphere changes during different years of solar activity, we study the occurrence of Es in response to solar variability. Figure 8 illustrates the occurrence of the Es layer in

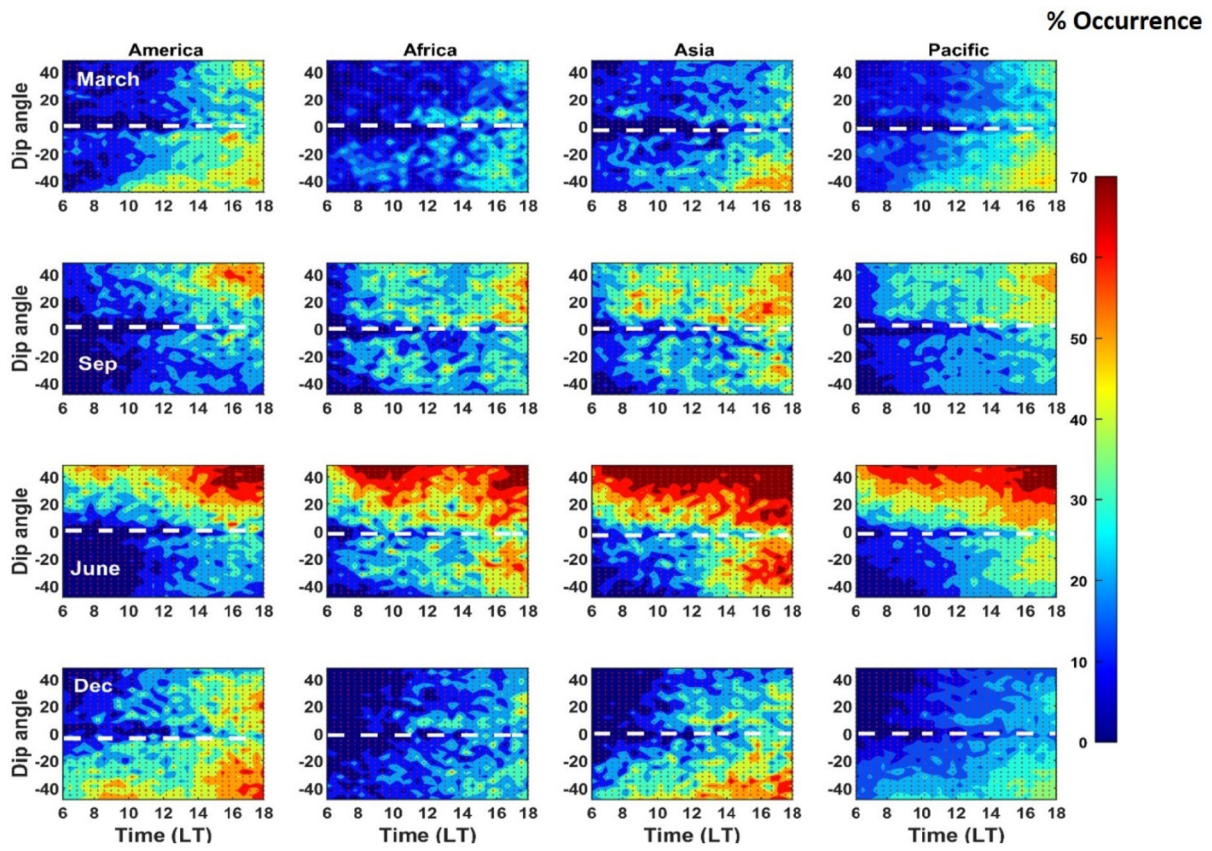


Fig. 4 The magnetic dip-LT distributions of Es occurrence for different longitude sectors (columns) and seasons (rows)

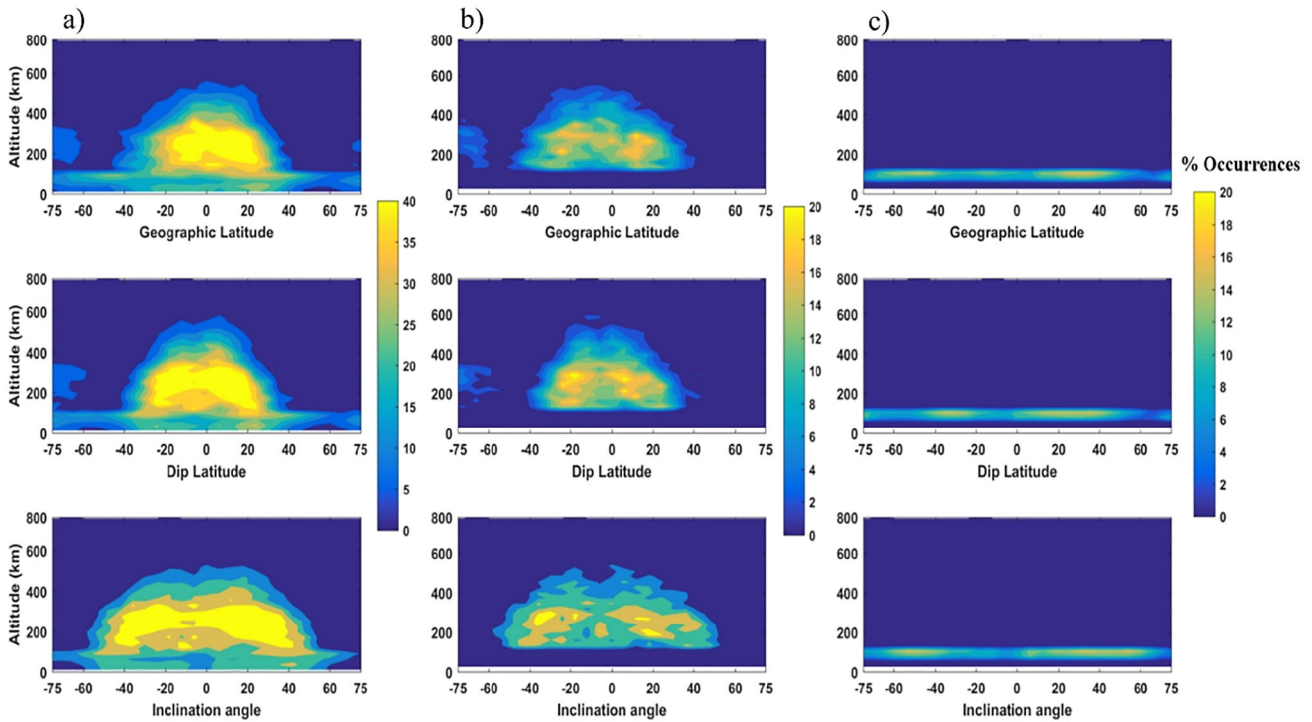
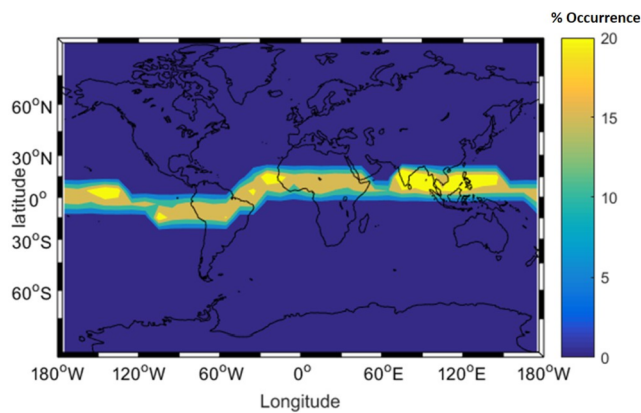
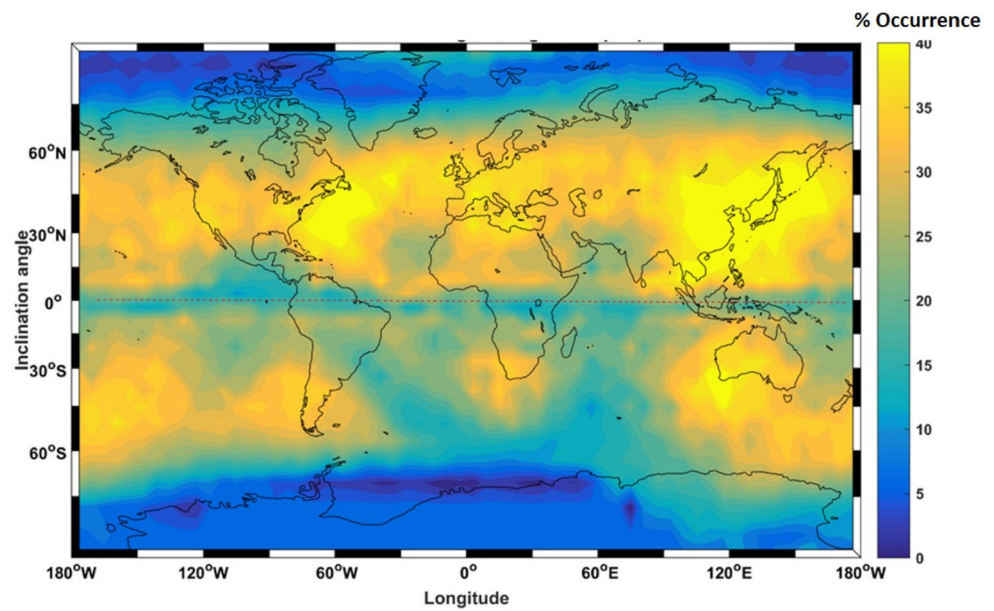


Fig. 5 a) Occurrence of scintillation as a function of Geographic latitude, dip latitude, and inclination angle (from above) obtained from GNSS RO from 2007 to 2013. b) Occurrence of scintillation above 200km as a function of Geographic latitude, dip latitude, and inclina-

tion angle (from above) obtained from GNSS RO. c) Occurrence of scintillation below 200 km as a function of Geographic latitude, dip latitude, and inclination angle (from above) obtained from GNSS RO



**Fig. 6** A global occurrence map of Es detected from COSMIC measurement in 2007-2013



**Fig. 7** Occurrence of Es along the magnetic dip equator ( $\pm 15^\circ$ ) as a function of geographic latitude and longitude

the Earth's ionosphere during various years of different solar activity cycles in 2007-2013. It is found from Fig. 8 that a negative correlation of the appearance probability of Es with solar activity is observed for intensive layers composed of metallic ions. This is in good agreement with the earlier studies (Bergsson and Syndergaard 2022; Fontes et al. 2024; Maksyutin et al. 2001; Maksyutin and Sherstyukov 2005).

Maksyutin et al. (2001) attributed the negative correlation with solar activity in case of intense Es layers having metal ions whereas the position correlation corresponds to weak Es layer with molecular ions. They also pointed the negative and positive correlations with the zonal and meridional winds, respectively. Extended studies were conducted later to demonstrating daytime positive correlation and nighttime negative correlations. With a huge database of Es recordings at low, mid and high latitude stations for a period of about 4 solar cycles, (Zhang et al. 2015) emphasized the fundamen-

tal role of the molecular and metallic ions for such opposite correlations during day and night. (Bergsson and Syndergaard 2022) explained the anticorrelation in terms of the varied occurrence altitude of the Es layer during different seasons that depends on solar activity. There are also other arguments that increased tidal wind amplitudes over the low latitudes during the low solar activity period are responsible for the Es layer formation and vice versa (Andrioli et al. 2022; Fontes et al. 2024).

## 4 Discussion

A summary of the Es occurrences using COSMIC RO scintillation data over an extended period of seven years has been given. The spatial and temporal characteristics of Es occurrences are analyzed for four longitude sectors, American, African, Asian and Pacific, for four seasons to establish the seasonal longitudinal occurrence of Es. Our observation from GNSS RO measurements clearly shows the occurrence of Es at the magnetic dip equator. In the following section, we describe the physical process of Es formation and the source mechanism of Es at the magnetic dip equator, where wind shear theory fails to operate. Earlier results of Chu et al. (2014) on global Es layer morphology through GPS RO measurements during the period 2006 to 2011 confirm that in the equatorial and low latitudes, Es layer occurrences have a weak correlation with the zonal wind shear. Similar studies were also conducted earlier to investigate the morphology of sporadic E layers on seasons through different constellations of RO observations (COSMIC, CHAMP and GRACE) along with wind shear measured by TIMED/TIDI, inferring maximum occurrence of Es in the summer hemisphere but could not explain the formation of Es layers and



Occurrence of the Es layer in the equatorial ionosphere during the period 2007-2013

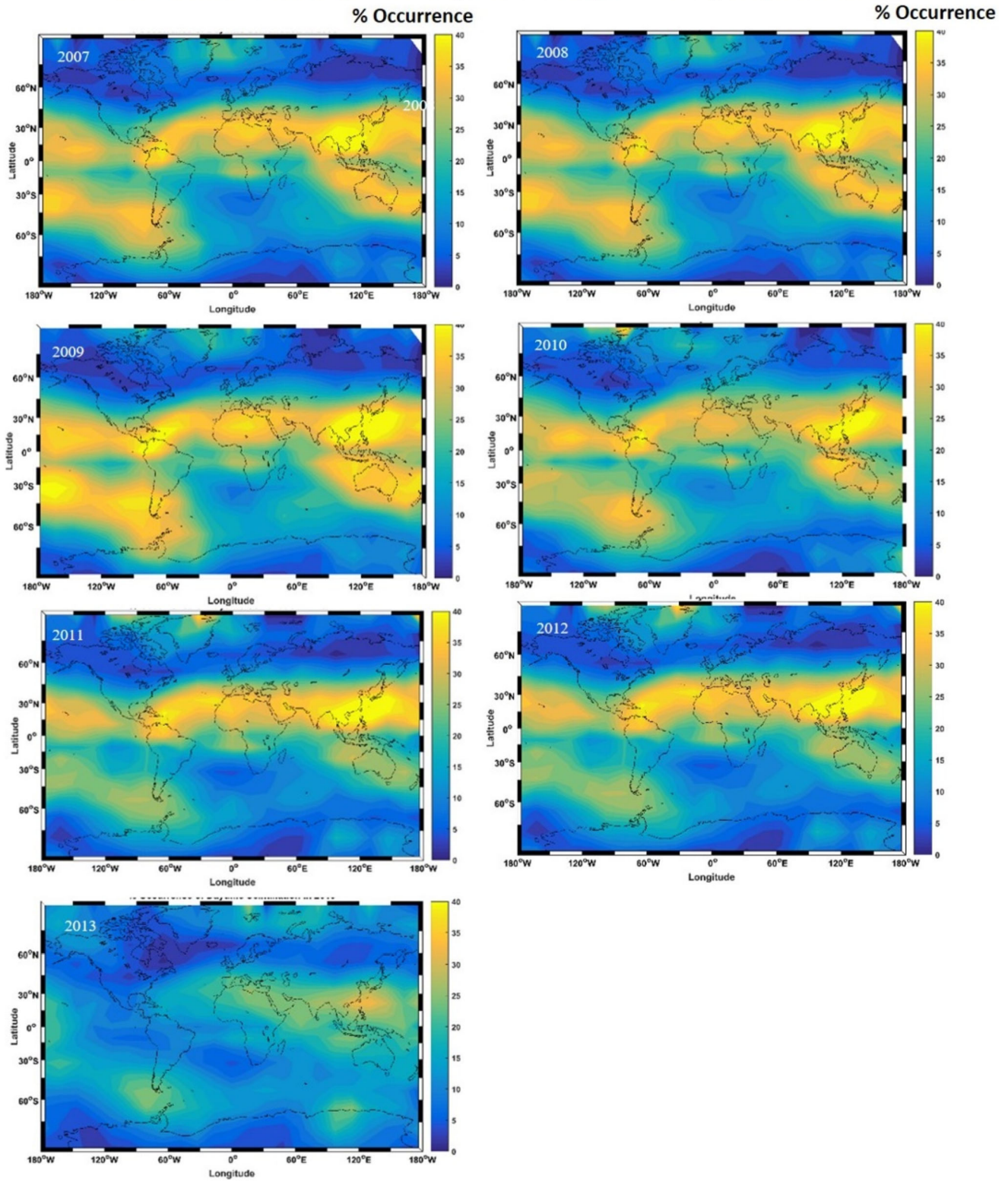
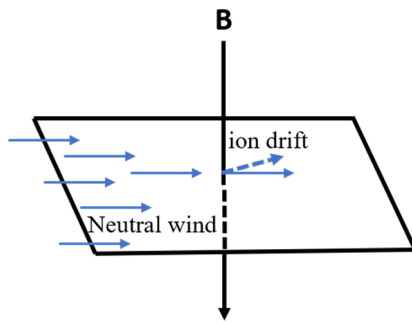


Fig. 8 Occurrence of the Es layer in the Earth’s ionosphere during different year from 2007 to 2013, referring to gradual increase in solar activity



**Fig. 9** The plot schematically illustrates the neutral wind moving perpendicular to the magnetic field  $B$  that causes a slightly tilted ion drift as represented in dashed arrow

its relation with wind shear at the equatorial region (Arras et al. 2008; Liu et al. 2018; Niu et al. 2019; Wu et al. 2005). Hence, the other mechanisms such as localization of magnetic field distribution, ionospheric electric fields, distribution of metallic ions and the chemical reactions therein could be explored (Shinagawa et al. 2017).

#### 4.1 Plasma instability mechanism for Es production at the magnetic dip equator

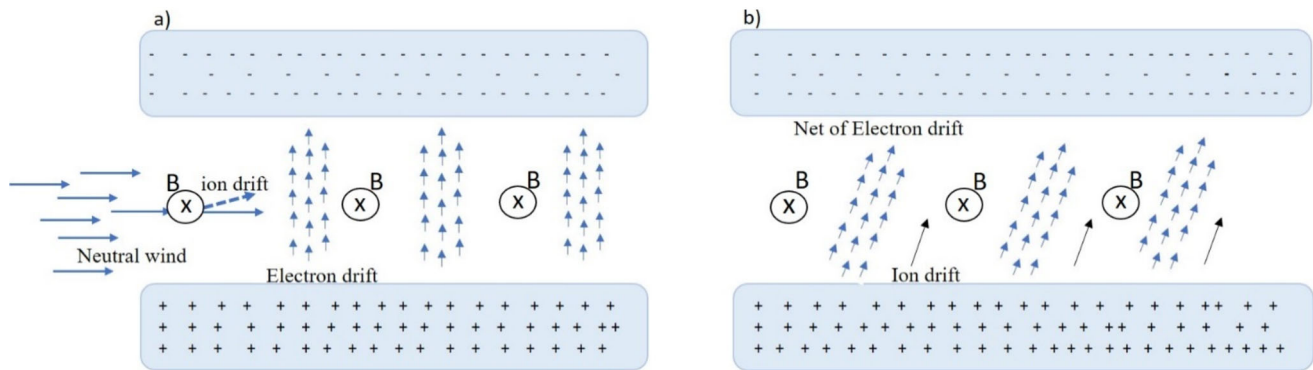
In order to comprehend the physical mechanisms and formation of Es at the magnetic dip equator, it is crucial to understand the plasma instability that occurs within the E-layer, where clusters of ions appear. To maintain charge neutrality, electrons are drawn towards these ion clusters. In the vicinity of the magnetic dip equator, there exists an ambient electric field perpendicular to the magnetic field. The magnetic field aligns in the north-south direction, while the electric field aligns in the east-west direction, as depicted in Fig. 10 (a). The Hall effect arises from this configuration, leading to the generation of a vertical electric field in the ionosphere. Simultaneously, the neutral wind, which is also perpendicular to the electric and magnetic fields, exerts a substantial influence on ions but has minimal impact on electrons (Whitehead 1997a,b). Consequently, when a neutral wind blows across the magnetic field, it primarily induces ion drift in the direction of the neutral wind, at nearly the same velocity. However, due to the influence of the magnetic field, these ion drifts exhibit a slight skewing (Whitehead 1997a), as illustrated in the sketch in Fig. 9.

Figure 10 provides a depiction of the ionosphere in the vicinity of the magnetic dip equator, illustrating the presence of a significant charge accumulation at the upper and lower side of the ionosphere. Close to the magnetic dip equator, the electron drift occurs vertically, while the magnetic fields are horizontal leading to the development of a strong electric field at the upper and lower side of the ionosphere (Forbes 1981; Whitehead 1997a,b). Since the magnetic field

is horizontal, the electrons are unable to travel along its direction to neutralize the charge (Whitehead 1997a). In order to prevent further charge build-up, the vertical electric field at the magnetic dip equator must be sufficiently powerful to drive ions at a speed comparable to the vertical electron drift. Simultaneously, the strong electric field induces a horizontal electron drift in the east-west direction, with a velocity significantly higher (around 10 times) than the ion drift. Consequently, there is a nearly 500 m/sec electron velocity drift, which is strong enough to trigger plasma instability (Whitehead 1970). Importantly, this effect is specific to the magnetic dip equator. When the vertical electric field reaches a certain strength (as shown in Figure 10b), ions move at a sufficient speed to keep up with the electron drift, thereby preventing further charge accumulation. The presence of this electric field amplifies the magnitude of the horizontal electron drift, leading to the initiation of instability (Whitehead 1997a). In essence, the relative drift between ions and electrons serves as a trigger for instability. The high-velocity electron drift generates plasma instability, causing electrons and ions to cluster into elongated, needle-shaped irregularities oriented in the north-south direction (Whitehead 1997b). These irregularities serve as the origin of the Es formation.

According to Seif et al. (2015) and Tsunoda (2008), another important aspect to consider is the influence of tidal winds on the equatorward transport of the Es layer. These winds have a downward-directed phase velocity, which means that in the absence of an electric field, the wind-shear node, where the Es layer resides, will move downwards. Consequently, if the downward transport persists, the Es layer will eventually reach an altitude where ion motion is predominantly affected by collisions with neutrals at that level. This leads to the ions becoming unmagnetized, making the  $U \times B$  (cross product of ion velocity and magnetic field) irrelevant.

When the wind-shear node reaches this altitude, the Es layer ceases to follow it and gets released at that specific altitude. This phenomenon, known as the corkscrew effect (Chimonas and Axford 1968), typically occurs at approximately 90-95 km altitude. However, it's worth noting that electrons remain magnetized during this process. The relative movement of electrons in comparison to ions generates the current responsible for driving the Gravity-Driven Instability (GDI). Once the Es layer is released at lower altitudes, it is no longer pushed out of the Equatorial Electrojet (EEJ) region by the  $E \times B$  drift ( $E_p$ ). Therefore, despite being dumped at low altitudes, the Es layer can still maintain the necessary gradient to trigger the GDI phenomenon. This is consistent with the earlier reports by different research groups (e.g., (Dhanya et al. 2008; Forbes 1981; Resende et al. 2016; Whitehead 1963)).



**Fig. 10** (a) Neutral wind perpendicular to the magnetic field causes a slight skew in ion drift (as shown in dashed arrow head). Additionally, vertical electron drift occurs, leading to the accumulation of a strong charge both above and below the ionosphere. (b) This strong electric field induces horizontal electron drift at a speed approximately

10 times faster than the original ion drift, reaching about 500 m/s. Such rapid electron drift induces plasma instability (Whitehead 1989). Consequently, high-speed electron drift leads to the formation of long, horizontal, needle-shaped irregularities as electrons and ions are bunched together

## 5 Conclusion

This paper provides a detailed analysis of Es recorded by the COSMIC satellites through the use of radio occultation (RO) over a period of seven years. The study identifies the dependence of Es occurrence rate on longitude, latitude, and season. It presents detailed characteristics of the spatial and temporal distribution of Es occurrence rate, particularly in regions that are not easily monitored by ground-based instruments, such as the peak occurrence during summer at middle latitudes, lower Es occurrence rate in America and the South Atlantic Anomaly region, low Es layer occurrences near the geomagnetic equator, and minimum Es occurrence rate in polar regions. Additionally, it provides observations at altitudes that cannot be continuously monitored through in situ observations from space-based platforms. The occurrence statistics of E-region irregularities (i.e., Es) in the COSMIC dataset align well with previous studies on Es found in the literature. The results indicate that factors like the horizontal intensity and inclination of the magnetic field contribute to the global distribution of Es layers. Importantly, solar maximum has a negative effect on the generation of Es and requires longer-term datasets for future investigations. We observe the occurrence of Es near the equatorial region where the magnetic field inclination approaches zero, the compression of electrons or ions is limited, resulting in a decreased Es occurrence rate in that area. Gradient Drift instability is proposed as a source mechanism of the appearance of Es at the magnetic dip equator, which is consistent with the previous studies that have been conducted by ground-based stations as mentioned in the discussion section. The study also examines the relationship between the Es occurrence rate and Earth's magnetic field, the effect of Earth's magnetic field has been discussed in previous studies (e.g. Luo et al. (2021)). Moreover, the huge number of

daily RO datasets over the low latitudes provided by the operating COSMIC-2 constellation of satellites opens further scopes for improving the understanding on global equatorial Sporadic-E occurrence characteristics.

**Acknowledgements** The authors would also like to thank the CDAAC of the University Corporation for Atmospheric Research (UCAR) for providing the COSMIC satellite observation data.

**Author contributions** A.S. and S.K.P. designed the conceptualization and methodology of the manuscript, processed the data and performed formal analysis and validated the results. A.S. prepared the initial manuscript and S.K.P. reviewed the manuscript. All authors read and approved the final manuscript.

**Funding** A. Seif gratefully acknowledges Iran's National Elites Foundation fund that was awarded to her to conduct this study. S. K. Panda acknowledges the Science & Engineering Research Board (SERB) (A statutory body of the Department of Science & Technology, Government of India) New Delhi, India, for the Core Research Grant (CRG) project vide File No: CRG/2019/003394.

**Data Availability** No datasets were generated or analysed during the current study.

## Declarations

**Competing interests** The authors declare no competing interests.

## References

- Alfonsi, L., Spogli, L., Pezzopane, M., Romano, V., Zuccheretti, E., De Franceschi, G., Cabrera, M.A., Ezquer, R.G.: Comparative analysis of spread-F signature and GPS scintillation occurrences at Tucumán, Argentina. *J. Geophys. Res. Space Phys.* **118**, 4483–4502 (2013). <https://doi.org/10.1002/jgra.50378>
- Andrioli, V.F., Xu, J., Batista, P.P., Resende, L.C.A., Da Silva, L.A., Marchezi, J.P., Li, H., Wang, C., Liu, Z., Guharay, A.: New findings relating tidal variability and solar activity in the low latitude MLT region. *J. Geophys. Res. Space Phys.* **127**, e2021JA030239 (2022). <https://doi.org/10.1029/2021JA030239>



- Arras, C.: A global survey of sporadic E layers based on GPS Radio occultations by CHAMP, GRACE and FORMOSAT-3/COSMIC (2010)
- Arras, C., Wickert, J.: Estimation of ionospheric sporadic E intensities from GPS radio occultation measurements. *J. Atmos. Sol.-Terr. Phys.* **171**, 60–63 (2018). <https://doi.org/10.1016/j.jastp.2017.08.006>
- Arras, C., Wickert, J., Beyerle, G., Heise, S., Schmidt, T., Jacobi, C.: A global climatology of ionospheric irregularities derived from GPS radio occultation. *Geophys. Res. Lett.* **35** (2008). <https://doi.org/10.1029/2008GL034158>
- Arras, C., Jacobi, C., Wickert, J.: Semidiurnal tidal signature in sporadic E occurrence rates derived from GPS radio occultation measurements at higher midlatitudes. *Ann. Geophys.* **27**, 2555–2563 (2009). <https://doi.org/10.5194/angeo-27-2555-2009>
- Arras, C., Resende, L.C.A., Kepkar, A., Senevirathna, G., Wickert, J.: Sporadic E layer characteristics at equatorial latitudes as observed by GNSS radio occultation measurements. *Earth Planets Space* **74**, 163 (2022). <https://doi.org/10.1186/s40623-022-01718-y>
- Axford, W.I.: The formation and vertical movement of dense ionized layers in the ionosphere due to neutral wind shears. *J. Geophys. Res.* **68**, 769–779 (1963). <https://doi.org/10.1029/JZ068i003p00769>
- Bergsson, B., Syndergaard, S.: Global temporal and spatial variations of ionospheric sporadic-E derived from radio occultation measurements. *J. Geophys. Res. Space Phys.* **127**, e2022JA030296 (2022). <https://doi.org/10.1029/2022JA030296>
- Brahmanandam, P.S., Uma, G., Liu, J.Y., Chu, Y.H., Latha Devi, N.S.M.P., Kakinami, Y.: Global S4 index variations observed using FORMOSAT-3/COSMIC GPS RO technique during a solar minimum year. *J. Geophys. Res. Space Phys.* **117** (2012). <https://doi.org/10.1029/2012JA017966>
- Carter, B.A., Zhang, K., Norman, R., Kumar, V.V., Kumar, S.: On the occurrence of equatorial F-region irregularities during solar minimum using radio occultation measurements. *J. Geophys. Res. Space Phys.* **118**, 892–904 (2013). <https://doi.org/10.1002/jgra.50089>
- Chandra, H., Rastogi, R.G.: Blanketing sporadic E layer near the magnetic equator. *J. Geophys. Res.* **80**, 149–153 (1975). <https://doi.org/10.1029/JA080i001p00149>
- Chimonas, G., Axford, W.I.: Vertical movement of temperate-zone sporadic E layers. *J. Geophys. Res.* **73**, 111–117 (1968). <https://doi.org/10.1029/JA073i001p00111>
- Chu, Y.H., Wang, C.Y., Wu, K.H., Chen, K.T., Tzeng, K.J., Su, C.L., Feng, W., Plane, J.M.C.: Morphology of sporadic E layer retrieved from COSMIC GPS radio occultation measurements: wind shear theory examination. *J. Geophys. Res. Space Phys.* **119**, 2117–2136 (2014). <https://doi.org/10.1002/2013JA019437>
- Coco, D.S., Gaussiran, T.L. II, Coker, C.: Passive detection of sporadic E using GPS phase measurements. *Radio Sci.* **30**, 1869–1874 (1995). <https://doi.org/10.1029/95RS02453>
- Collinson, G.A., McFadden, J., Grebowsky, J., Mitchell, D., Lillis, R., Withers, P., Vogt, M.F., Benna, M., Espley, J., Jakosky, B.: Constantly forming sporadic E-like layers and rifts in the Martian ionosphere and their implications for Earth. *Nat. Astron.* **4**, 486–491 (2020). <https://doi.org/10.1038/s41550-019-0984-8>
- Devasia, C.V.: Blanketing sporadic-E characteristics at the equatorial stations Trivandrum & Kodaikanal. (1976)
- Dhanya, R., Gurubaran, S., Emperumal, K.: Lower E-region echoes over the magnetic equator as observed by the MF radar at Tirunelveli (8.7° N, 77.8° E) and their relationship to Esq and Esb. *Ann. Geophys.* **26**, 2459–2470 (2008). <https://doi.org/10.5194/angeo-26-2459-2008>
- Emmons, D.J., Wu, D.L., Swarnalingam, N., Ali, A.F., Ellis, J.A., Fitch, K.E., Obenberger, K.S.: Improved models for estimating sporadic-E intensity from GNSS radio occultation measurements. *Front. Astron. Space Sci.* **10** (2023). <https://doi.org/10.3389/fspas.2023.1327979>
- Farley, D.T.: Theory of equatorial electrojet plasma waves: new developments and current status. *J. Atmos. Terr. Phys.* **47**, 729–744 (1985). [https://doi.org/10.1016/0021-9169\(85\)90050-9](https://doi.org/10.1016/0021-9169(85)90050-9)
- Fontes, P.A., Muella, M.T.A.H., Resende, L.C.A., Fagundes, P.R.: Evidence of anti-correlation between sporadic (Es) layers occurrence and solar activity observed at low latitudes over the Brazilian sector. *Adv. Space Res.* **73**, 3563–3577 (2024). <https://doi.org/10.1016/j.asr.2023.09.040>
- Forbes, J.M.: The equatorial electrojet. *Rev. Geophys.* **19**, 469–504 (1981). <https://doi.org/10.1029/RG019i003p00469>
- Fujita, M., Ogawa, T., Koike, K.: 1.7 GHz scintillation measurements at midlatitude using a geostationary satellite beacon. *J. Atmos. Terr. Phys.* **40**, 963–968 (1978). [https://doi.org/10.1016/0021-9169\(78\)90149-6](https://doi.org/10.1016/0021-9169(78)90149-6)
- Hajkowicz, L.A.: Multi-satellite scintillations, spread-F and sporadic-E over Brisbane—1. *J. Atmos. Terr. Phys.* **39**, 359–365 (1977). [https://doi.org/10.1016/S0021-9169\(77\)90150-7](https://doi.org/10.1016/S0021-9169(77)90150-7)
- Hajkowicz, L.A.: Multi-satellite scintillations, spread-F and sporadic-E over Brisbane — 2. *J. Atmos. Terr. Phys.* **40**, 99–104 (1978). [https://doi.org/10.1016/0021-9169\(78\)90113-7](https://doi.org/10.1016/0021-9169(78)90113-7)
- Hajkowicz, L.A., Minakoshi, H.: Mid-latitude ionospheric scintillation anomaly in the Far East. *Ann. Geophys.* **21**, 577–581 (2003). <https://doi.org/10.5194/angeo-21-577-2003>
- Haldoupis, C.: A tutorial review on sporadic E layers. In: Abdu, M.A., Pancheva, D. (eds.) *Aeronomy of the Earth's Atmosphere and Ionosphere*, pp. 381–394. Springer, Dordrecht (2011)
- Haldoupis, C., Pancheva, D.: Terdiurnal tidelike variability in sporadic E layers. *J. Geophys. Res. Space Phys.* **111** (2006). <https://doi.org/10.1029/2005JA011522>
- Hocke, K.K., Igarashi, K., Nakamura, M., Wilkinson, P., Wu, J., Pavelyev, A., Wickert, J.: Global sounding of sporadic E layers by the GPS/MET radio occultation experiment. *J. Atmos. Sol.-Terr. Phys.* **63**, 1973–1980 (2001). [https://doi.org/10.1016/S1364-6826\(01\)00063-3](https://doi.org/10.1016/S1364-6826(01)00063-3)
- Hodos, T.J., Nava, O.A., Dao, E.V., Emmons, D.J.: Global sporadic-E occurrence rate climatology using GPS radio occultation and ionosonde data. *J. Geophys. Res. Space Phys.* **127**, e2022JA030795 (2022). <https://doi.org/10.1029/2022JA030795>
- Huang, Y.: Ionospheric scintillations at lunping. *J. Chin. Inst. Eng.* **1**, 81–84 (1978). <https://doi.org/10.1080/02533839.1978.9676618>
- Huang, C.-S.: Effects of the postsunset vertical plasma drift on the generation of equatorial spread F. *Prog. Earth Planet. Sci.* **5**, 3 (2018). <https://doi.org/10.1186/s40645-017-0155-4>
- Jeng-Shing Chern, R., Huang, C.-M.: Effect of orbit inclination on the performance of FORMOSAT-3/7 type constellations. *Acta Astronaut.* **82**, 47–53 (2013). <https://doi.org/10.1016/j.actaastro.2012.05.005>
- Jiao, Y., Hall, J.J., Morton, Y.T.: Performance evaluation of an automatic GPS ionospheric phase scintillation detector using a machine-learning algorithm. *Navigation* **64**, 391–402 (2017). <https://doi.org/10.1002/navi.188>
- Juang, J.-C., Tsai, Y.-F., Chu, C.-H.: On constellation design of multi-GNSS radio occultation mission. *Acta Astronaut.* **82**, 88–94 (2013). <https://doi.org/10.1016/j.actaastro.2012.04.031>
- Kelly, M.: *The Earth's Ionosphere: Plasma Physics and Electrodynamics*. Elsevier, Amsterdam (2012)
- Kirkwood, S., Nilsson, H.: High-latitude sporadic-E and other thin layers – the role of magnetospheric electric fields. *Space Sci. Rev.* **91**, 579–613 (2000). <https://doi.org/10.1023/A:1005241931650>
- Ko, C.P., Yeh, H.C.: COSMIC/FORMOSAT-3 observations of equatorial F region irregularities in the SAA longitude sector. *J. Geophys. Res. Space Phys.* **115** (2010). <https://doi.org/10.1029/2010JA015618>
- Kumar, S., Kishore, A., Ramachandran, V.: Ionospheric scintillations on 3.925 GHz signal from Intelsat (701) at low latitude in the

- South Pacific region. *Phys. Scr.* **75**, 258 (2007). <https://doi.org/10.1088/0031-8949/75/3/005>
- Langley, R.B.: GPS, the ionosphere, and the solar maximum. *GPS World* **11**, 44–49 (2000)
- Leighton, H.I., Shapley, A.H., Smith, E.K.: The occurrence of sporadic E during the IGY. In: Smith, E.K., Matsushita, S. (eds.) *Ionospheric Sporadic*, pp. 166–177. Pergamon, Elmsford (1962)
- Li, Q.B., Huang, Z., Chen, S.: A statistical analysis of global ionospheric E-layer scintillation during 2007–2014. *Radio Sci.* **55**, e2018RS006764 (2020). <https://doi.org/10.1029/2018RS006764>
- Liu, C.L., Kirchengast, G., Zhang, K., Norman, R., Li, Y., Zhang, S.C., Fritzer, J., Schwaerz, M., Wu, S.Q., Tan, Z.X.: Quantifying residual ionospheric errors in GNSS radio occultation bending angles based on ensembles of profiles from end-to-end simulations. *Atmos. Meas. Tech.* **8**, 2999–3019 (2015). <https://doi.org/10.5194/amt-8-2999-2015>
- Liu, Y., Zhou, C., Tang, Q., Li, Z., Song, Y., Qing, H., Ni, B., Zhao, Z.: The seasonal distribution of sporadic E layers observed from radio occultation measurements and its relationship with wind shear measured by TIMED/TIDI. *Adv. Space Res.* **62**, 426–439 (2018). <https://doi.org/10.1016/j.asr.2018.04.026>
- Luo, J., Liu, H., Xu, X.: Sporadic E morphology based on COSMIC radio occultation data and its relationship with wind shear theory. *Earth Planets Space* **73**, 212 (2021). <https://doi.org/10.1186/s40623-021-01550-w>
- MacDougall, J.W., Jayachandran, P.T., Plane, J.M.C.: Polar cap sporadic-E: part 1, observations. *J. Atmos. Sol.-Terr. Phys.* **62**, 1155–1167 (2000a). [https://doi.org/10.1016/S1364-6826\(00\)00093-6](https://doi.org/10.1016/S1364-6826(00)00093-6)
- MacDougall, J.W., Plane, J.M.C., Jayachandran, P.T.: Polar cap sporadic-E: part 2, modeling. *J. Atmos. Sol.-Terr. Phys.* **62**, 1169–1176 (2000b). [https://doi.org/10.1016/S1364-6826\(00\)00092-4](https://doi.org/10.1016/S1364-6826(00)00092-4)
- Macmillan, S., Maus, S.: International geomagnetic reference field—the tenth generation. *Earth Planets Space* **57**, 1135–1140 (2005). <https://doi.org/10.1186/BF03351896>
- Maksyutin, S.V., Sherstyukov, O.N.: Dependence of E-sporadic layer response on solar and geomagnetic activity variations from its ion composition. *Adv. Space Res.* **35**, 1496–1499 (2005). <https://doi.org/10.1016/j.asr.2005.05.062>
- Maksyutin, S.V., Sherstyukov, O.N., Fahrutdinova, A.N.: Dependence of sporadic-E layer and lower thermosphere dynamics on solar activity. *Adv. Space Res.* **27**, 1265–1270 (2001). [https://doi.org/10.1016/S0273-1177\(01\)00195-8](https://doi.org/10.1016/S0273-1177(01)00195-8)
- Mao, X., Visser, P.N.A.M., van den IJssel, J.: The impact of GPS receiver modifications and ionospheric activity on Swarm baseline determination. *Acta Astronaut.* **146**, 399–408 (2018). <https://doi.org/10.1016/j.actaastro.2018.03.009>
- Mathews, J.D.: Sporadic E: current views and recent progress. *J. Atmos. Sol.-Terr. Phys.* **60**, 413–435 (1998). [https://doi.org/10.1016/S1364-6826\(97\)00043-6](https://doi.org/10.1016/S1364-6826(97)00043-6)
- Mathews, J.D., Bekeney, F.S.: Upper atmosphere tides and the vertical motion of ionospheric sporadic layers at Arecibo. *J. Geophys. Res. Space Phys.* **84**, 2743–2750 (1979). <https://doi.org/10.1029/JA084iA06p02743>
- Niu, J., Fang, H.: An empirical model of the sporadic E layer intensity based on COSMIC radio occultation observations. *Space Weather* **21**, e2022SW003280 (2023). <https://doi.org/10.1029/2022SW003280>
- Niu, J., Weng, L.B., Meng, X., Fang, H.X.: Morphology of ionospheric sporadic E layer intensity based on COSMIC occultation data in the midlatitude and low-latitude regions. *J. Geophys. Res. Space Phys.* **124**, 4796–4808 (2019). <https://doi.org/10.1029/2019JA026828>
- Ogawa, T., Suzuki, A., Kunitake, M.: Spatial distribution of midlatitude sporadic E scintillations in summer daytime. *Radio Sci.* **24**, 527–538 (1989). <https://doi.org/10.1029/RS024i004p00527>
- Oyinloye, J.O.: A study of blanketing sporadic E in the equatorial region. *Planet. Space Sci.* **19**, 1131–1139 (1971). [https://doi.org/10.1016/0032-0633\(71\)90109-7](https://doi.org/10.1016/0032-0633(71)90109-7)
- Panda, S.K., Haralambous, H., Moses, M., Dabbakuti, J.R.K.K., Tariku, Y.A.: Ionospheric and plasmaspheric electron contents from space-time collocated digisonde, COSMIC, and GPS observations and model assessments. *Acta Astronaut.* **179**, 619–635 (2021). <https://doi.org/10.1016/j.actaastro.2020.12.005>
- Patel, K., Singh, A.K., Patel, R.P., Singh, R.P.: Ionospheric scintillations by sporadic-E irregularities over low latitude. *Bull. Astron. Soc. India* **35**, 625–630 (2007)
- Patel, K., Singh, A.K., Patel, R.P., Singh, R.P.: Characteristics of low latitude ionospheric E-region irregularities linked with daytime VHF scintillations measured from Varanasi. *J. Earth Syst. Sci.* **118**, 721–732 (2009). <https://doi.org/10.1007/s12040-009-0058-x>
- Qiu, L., Yu, T., Yan, X., Sun, Y.-Y., Zuo, X., Yang, N., Wang, J., Qi, Y.: Altitudinal and latitudinal variations in ionospheric sporadic-E layer obtained from FORMOSAT-3/COSMIC radio occultation. *J. Geophys. Res. Space Phys.* **126**, e2021JA029454 (2021). <https://doi.org/10.1029/2021JA029454>
- Reddy, C.A., Devasia, C.V.: VHF radar observations of gradient instabilities associated with blanketing Es layers in the equatorial electrojet. *J. Geophys. Res.* **82**, 125–128 (1977). <https://doi.org/10.1029/JA082i001p00125>
- Resende, L.C.A., Batista, I.S., Denardini, C.M., Carrasco, A.J., de Fátima Andrioli, V., Moro, J., Batista, P.P., Chen, S.S.: Competition between winds and electric fields in the formation of blanketing sporadic E layers at equatorial regions. *Earth Planets Space* **68**, 201 (2016). <https://doi.org/10.1186/s40623-016-0577-z>
- Resende, L.C.A., Arras, C., Batista, I.S., Denardini, C.M., Bertolotto, T.O., Moro, J.: Study of sporadic E layers based on GPS radio occultation measurements and digisonde data over the Brazilian region. *Ann. Geophys.* **36**, 587–593 (2018a). <https://doi.org/10.5194/angeo-36-587-2018>
- Resende, L.C.A., Batista, I.S., Denardini, C.M., Batista, P.P., Carrasco, A.J., Andrioli, V.F., Moro, J.: The influence of tidal winds in the formation of blanketing sporadic e-layer over equatorial Brazilian region. *J. Atmos. Sol.-Terr. Phys.* **171**, 64–71 (2018b). <https://doi.org/10.1016/j.jastp.2017.06.009>
- Rocken, C., Ying-Hwa, K., Schreiner, W.S., Hunt, D., Sokolovskiy, S., McCormick, C.: COSMIC system description. *Terr. Atmos. Ocean. Sci.* **11**, 21–52 (2000)
- Seif, A., Abdullah, M., Marie Hasbi, A., Zou, Y.: Investigation of ionospheric scintillation at UKM station, Malaysia during low solar activity. *Acta Astronaut.* **81**, 92–101 (2012). <https://doi.org/10.1016/j.actaastro.2012.06.024>
- Seif, A., Tsunoda, R.T., Abdullah, M., Hasbi, A.M.: Daytime gigahertz scintillations near magnetic equator: relationship to blanketing sporadic E and gradient-drift instability. *Earth Planets Space* **67**, 177 (2015). <https://doi.org/10.1186/s40623-015-0348-2>
- Seif, A., Liu, J.-Y., Mannucci, A.J., Carter, B.A., Norman, R., Caton, R.G., Tsunoda, R.T.: A study of daytime L-band scintillation in association with sporadic E along the magnetic dip equator. *Radio Sci.* **52**, 1570–1577 (2017). <https://doi.org/10.1002/2017RS006393>
- Shinagawa, H., Miyoshi, Y., Jin, H., Fujiwara, H.: Global distribution of neutral wind shear associated with sporadic E layers derived from GAIA. *J. Geophys. Res. Space Phys.* **122**, 4450–4465 (2017). <https://doi.org/10.1002/2016JA023778>
- Sinno, K.: Ionospheric scintillation and fluctuation of Faraday rotation caused by spread-F and sporadic-E over Kokubunji, Japan (1980)
- Spilker, J.J. Jr: GPS signal structure and performance characteristics. *Navigation* **25**, 121–146 (1978)
- Syndergaard, S.: COSMIC S4 Data, COSMIC Data Analysis and Archival. Center at UCAR (2006)

- Tang, Q., Zhou, C., Liu, H., Liu, Y., Zhao, J., Yu, Z., Zhao, Z., Feng, X.: Latitudinal dependence of the geomagnetic and solar activity effect on sporadic-E layer. *Atmos. Chem. Phys. Discuss.* **2022**, 1–18 (2022). <https://doi.org/10.5194/acp-2022-534>
- Timoçin, E., Inyurt, S., Temuçin, H., Ansari, K., Jamjareegulgarn, P.: Investigation of equatorial plasma bubble irregularities under different geomagnetic conditions during the equinoxes and the occurrence of plasma bubble suppression. *Acta Astronaut.* **177**, 341–350 (2020). <https://doi.org/10.1016/j.actaastro.2020.08.007>
- Tsai, L.-C., Su, S.-Y., Liu, C.-H., Schuh, H., Wickert, J., Alizadeh, M.M.: Global morphology of ionospheric sporadic E layer from the FormoSat-3/COSMIC GPS radio occultation experiment. *GPS Solut.* **22**, 118 (2018). <https://doi.org/10.1007/s10291-018-0782-2>
- Tsunoda, R.T.: On blanketing sporadic E and polarization effects near the equatorial electrojet. *J. Geophys. Res. Space Phys.* **113** (2008). <https://doi.org/10.1029/2008JA013158>
- Vankadara, R.K., Panda, S.K., Amory-Mazaudier, C., Fleury, R., Devanaboyina, V.R., Pant, T.K., Jamjareegulgarn, P., Haq, M.A., Okoh, D., Seemala, G.K.: Signatures of Equatorial Plasma Bubbles and Ionospheric Scintillations from Magnetometer and GNSS Observations in the Indian Longitudes during the Space Weather Events of Early September 2017. *Remote Sens.* **14** (2022). <https://doi.org/10.3390/rs14030652>
- Whitehead, J.D.: The formation of the sporadic-E layer in the temperate zones. *J. Atmos. Terr. Phys.* **20**, 49–58 (1961). [https://doi.org/10.1016/0021-9169\(61\)90097-6](https://doi.org/10.1016/0021-9169(61)90097-6)
- Whitehead, J.D.: Theory of equatorial sporadic-E. *J. Atmos. Terr. Phys.* **25**, 167–173 (1963)
- Whitehead, J.D.: Production and prediction of sporadic E. *Rev. Geophys.* **8**, 65–144 (1970). <https://doi.org/10.1029/RG008i001p00065>
- Whitehead, J.D.: Recent work on mid-latitude and equatorial sporadic-E. *J. Atmos. Terr. Phys.* **51**, 401–424 (1989). [https://doi.org/10.1016/0021-9169\(89\)90122-0](https://doi.org/10.1016/0021-9169(89)90122-0)
- Whitehead, D.: Sporadic E-A mystery solved?: part 1-untangling the vagaries of sporadic-E propagation, and exploring a new hypothesis. *QST-NEWINGTON-* **81**, 39–41 (1997a)
- Whitehead, D.: Sporadic E-A mystery solved?: part 2-untangling the vagaries of sporadic-E propagation, and exploring a new hypothesis. *QST-NEWINGTON-* **81**, 38–42 (1997b)
- Wu, D.L., Ao, C.O., Hajj, G.A., de la Torre Juarez, M., Mannucci, A.J.: Sporadic E morphology from GPS-CHAMP radio occultation. *J. Geophys. Res. Space Phys.* **110** (2005). <https://doi.org/10.1029/2004JA010701>
- Yakovlev, O.I., Wickert, J., Pavelyev, A.G., Matyugov, S.S., Anufriev, V.A.: Sporadic structures in equatorial ionosphere as revealed from GPS occultation data. *Acta Astronaut.* **63**, 1350–1359 (2008). <https://doi.org/10.1016/j.actaastro.2008.05.023>
- Yakovlev, O.I., Wickert, J., Pavelyev, A.G., Cherkunova, G.P., Anufriev, V.A.: Results of radio occultation measurement of polar ionosphere at satellite-to-satellite paths during strong flare solar activity. *Acta Astronaut.* **67**, 315–323 (2010). <https://doi.org/10.1016/j.actaastro.2010.02.017>
- Yamazaki, Y., Arras, C., Andoh, S., Miyoshi, Y., Shinagawa, H., Harding, B.J., Englert, C.R., Immel, T.J., Sobkhiz-Miandehi, S., Stolle, C.: Examining the wind shear theory of sporadic E with ICON/MIGHTI winds and COSMIC-2 radio occultation data. *Geophys. Res. Lett.* **49**, e2021GL096202 (2022). <https://doi.org/10.1029/2021GL096202>
- Yu, B., Xue, X., Yue, X., Yang, C., Yu, C., Dou, X., Ning, B., Hu, L.: The global climatology of the intensity of the ionospheric sporadic E layer. *Atmos. Chem. Phys.* **19**, 4139–4151 (2019). <https://doi.org/10.5194/acp-19-4139-2019>
- Yu, B., Scott, C.J., Xue, X., Yue, X., Dou, X.: Derivation of global ionospheric sporadic E critical frequency (foEs) data from the amplitude variations in GPS/GNSS radio occultations. *R. Soc. Open Sci.* **7**, 200320 (2020). <https://doi.org/10.1098/rsos.200320>
- Yu, B., Xue, X., Scott, C.J., Yue, X., Dou, X.: An empirical model of the ionospheric sporadic E layer based on GNSS radio occultation data. *Space Weather* **20**, e2022SW003113 (2022). <https://doi.org/10.1029/2022SW003113>
- Yue, X., Schreiner, W.S., Zeng, Z., Kuo, Y.-H., Xue, X.: Case study on complex sporadic E layers observed by GPS radio occultations. *Atmos. Meas. Tech.* **8**, 225–236 (2015). <https://doi.org/10.5194/amt-8-225-2015>
- Yue, X., Schreiner, W.S., Pedatella, N.M., Kuo, Y.-H.: Characterizing GPS radio occultation loss of lock due to ionospheric weather. *Space Weather* **14**, 285–299 (2016). <https://doi.org/10.1002/2015SW001340>
- Zhang, Y., Wu, J., Guo, L., Hu, Y., Zhao, H., Xu, T.: Influence of solar and geomagnetic activity on sporadic-E layer over low, mid and high latitude stations. *Adv. Space Res.* **55**, 1366–1371 (2015). <https://doi.org/10.1016/j.asr.2014.12.010>
- Zou, Y.: Ionospheric scintillations at Guilin detected by GPS ground-based and radio occultation observations. *Adv. Space Res.* **47**, 945–965 (2011). <https://doi.org/10.1016/j.asr.2010.11.016>
- Zou, Y., Wang, D.: A study of GPS ionospheric scintillations observed at Guilin. *J. Atmos. Sol.-Terr. Phys.* **71**, 1948–1958 (2009). <https://doi.org/10.1016/j.jastp.2009.08.005>

**Publisher's Note** Springer Nature remains neutral with regard to jurisdictional claims in published maps and institutional affiliations.

Springer Nature or its licensor (e.g. a society or other partner) holds exclusive rights to this article under a publishing agreement with the author(s) or other rightsholder(s); author self-archiving of the accepted manuscript version of this article is solely governed by the terms of such publishing agreement and applicable law.